PROCEEDINGS OF SCIENCE

Topology of the $O(3)$ non-linear sigma model under the gradient flow

Stuart Thomas[a,*] **and Christopher Monahan**[a,b]

[a] *Department of Physics, William & Mary, Williamsburg, Virginia 23187, USA*

[b] *Thomas Jefferson National Accelerator Facility, Newport News, Virginia, USA*

E-mail: snthomas01@email.wm.edu, cjmonahan@wm.edu

The $O(3)$ non-linear sigma model (NLSM) is a prototypical field theory for QCD and ferromagnetism, featuring topological qualities. Though the topological susceptibility χ_t should vanish in physical theories, lattice simulations of the NLSM find that χ_t diverges in the continuum limit. We study the effect of the gradient flow on this quantity using a Markov Chain Monte Carlo method, finding that a logarithmic divergence persists. This result supports a previous study and indicates that either the definition of topological charge is problematic or the NLSM has no well-defined continuum limit. We also introduce a θ-term and analyze the topological charge as a function of θ under the gradient flow.

The 38th International Symposium on Lattice Field Theory, LATTICE2021 26th-30th July, 2021 Zoom/Gather@Massachusetts Institute of Technology

*Speaker

https://pos.sissa.it/

1. Introduction

Spin models provide a framework for understanding the physics of strongly-coupled systems, from solid state and condensed matter systems to nuclear and particle physics. The non-linear sigma model (NLSM), in particular, has provided a rich arena in which to study nonperturbative effects. In solid-state systems, this model describes Heisenberg ferromagnets [1] and in nuclear physics, it acts as a prototype for quantum chromodynamics (QCD), the gauge theory of the strong nuclear force. In general, the NLSM shares key features with non-Abelian gauge theories such as QCD, including a mass gap and asymptotic freedom [2], and has proved a useful model for exploring the effect of these properties in a simpler system.

We consider the $O(3)$ NLSM in 1+1 dimensions (one dimension of space, one dimension of time). This theory exhibits topological properties, such as *instantons*, or classical field solutions at local minima of the action in Euclidean space. These topologically protected solutions cannot evolve into the vacuum state via local fluctuations. This property has become critically important to quantum field theories in cosmology and high energy physics [3]. CJM: Can we provide a more explicit example(s) here? Statement is very vague at the moment. Additionally, topological stability may become a key tool for fault-tolerant quantum computers [4]. In these devices, topology protects the delicate quantum states necessary for information processing.

2. The Non-Linear Sigma Model

We study the $O(3)$ NLSM in two dimensions CJM: [In Euclidean space it does not really make sense to distinguish time and space, unless we start in Minkowski spacetime and then Wick rotate.], defined by the Euclidean action

$$S_E = \frac{\beta}{2} \int d^2x \, \left[(\partial_t \vec{e}\,)^2 + (\partial_x \vec{e}\,)^2 \right],$$

where $\vec{e}$ is 3-component real vector constrained by $|\vec{e}\,| = 1$ and β is the inverse coupling constant.

Following [5], we define the topological charge density, $q(x^*)$, for each plaquette x^* such that the total topological charge is

$$Q = \sum_{x^*} q(x^*), \tag{1}$$

where

$$q(x^*) = \frac{1}{4\pi} \left[A\Big(\vec{e}(x_1), \vec{e}(x_2), \vec{e}(x_3)\Big) + A\Big(\vec{e}(x_1), \vec{e}(x_3), \vec{e}(x_4)\Big) \right]. \tag{2}$$

Here A is the signed area of the triangle in target space, which we represent in the left-hand figure of Fig. 1. This value is defined if $A \neq 0, 2\pi$, or in other words, as long as the three points on the sphere are distinct and do not form a hemisphere. In numerical calculations, these points can be ignored. Therefore, we impose that the signed area is defined on the smallest spherical triangle, or $-2\pi < A < 2\pi$.

CJM: Need text here to explain the next equations

$$S[\vec{e}\,] \to S[\vec{e}\,] - i\theta Q[\vec{e}\,].$$

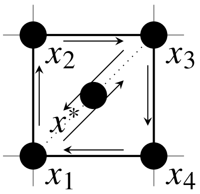

(a) Visualization of a plaquette x^*. The dotted line separates the plaquette into two signed areas, used to define the topological charge density $q(x^*)$. Arrows represent the order of signed area.

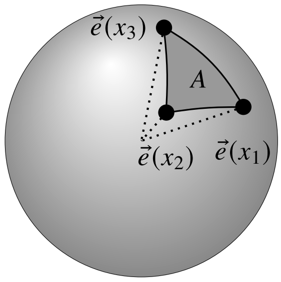

(b) The signed area of a triangle in target space.

Figure 1

A nonzero θ implies nonzero $\langle Q \rangle$. Furthermore,

$$\chi_t \propto \left. \frac{d\,\mathrm{Im}\langle Q \rangle}{d\theta} \right|_{\theta=0} \tag{3}$$

We define the topological susceptibility χ_t

$$\chi_t \equiv \frac{1}{L^2}\Big(\langle Q^2 \rangle - \langle Q \rangle^2\Big). \tag{4}$$

In the trivial case, $\langle Q \rangle$ is equal to 0 and on this lattice, this becomes

$$\chi_t = \frac{1}{L^2}\sum_{x^*,y^*}\langle q(x^*)q(y^*)\rangle = \frac{1}{L^2}\sum_{x^*}\langle q(x^*)q(0)\rangle, \tag{5}$$

where in the second equality we have assumed periodic boundary conditions. The topological susceptibility diverges in the continuum limit owing solely to the $x^* = 0$ term [6]. This divergence exists in QCD as well [**?**].

2.1 Gradient flow

CJM: Sentences/paragraph introducing continuous gradient flow here

3. Numerical implementation

We implement a numerical Monte Carlo method to study the NLSM in two dimensions using the discretized action

$$S_{\text{lat}}[\vec{e}\,] = \sum_i \left[2 - \vec{e}(x + a\hat{t}\,)\cdot\vec{e}(x) - \vec{e}(x + a\hat{x})\cdot\vec{e}(x)\right]. \tag{6}$$

We generate configurations using the Metropolis [] and Wolff cluster [**?**] algorithms, implemented in C++ and parallelized through the Message Passing Interface with a checkerboard algorithm [].

We thermalize the configurations with 1000 sweeps, with a cluster update every five sweeps, and illustrate a sample Markov chain in Fig. 2, where we plot the action as a function of Metropolis sweeps. We use Wolff's automatic windowing procedure [**?**] to estimate the autocorrelation times

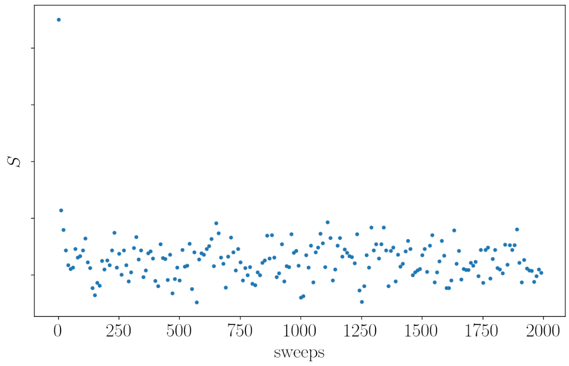

(a) $L = 24$

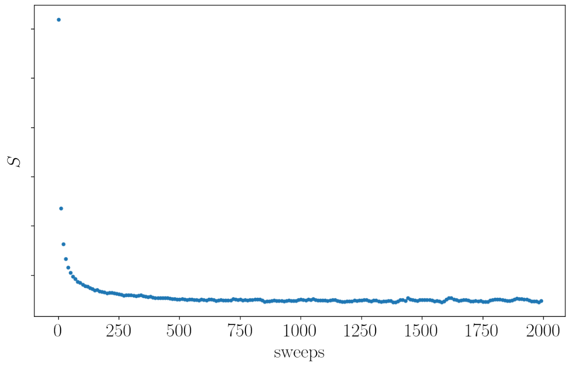

(b) $L = 404$

Figure 2: Plots of the action as a function of Monte Carlo time, starting with a random NLSM lattice.

for various observables, such as the magnetic susceptibility χ_m. We measure observables every 50 sweeps for each simulation.

We apply the gradient flow equation

$$\partial_\tau \vec{e}(\tau, x) = \left(1 - \vec{e}(\tau, x)\vec{e}(\tau, x)^T\right) \partial^2 \vec{e}(\tau, x), \tag{7}$$

where the Laplacian operator ∂^2 is defined as

$$\partial^2 \vec{e}(\tau, x) = \vec{e}(\tau, x + a\hat{t}) + \vec{e}(\tau, x - a\hat{t}) + \vec{e}(\tau, x + a\hat{x}) + \vec{e}(\tau, x - a\hat{x}) - 4\vec{e}(t, x).$$

We numerically solve the ordinary differential equation in Eq. 7 using a fourth-order Runga-Kutta approximation. To increase the efficiency of this algorithm, we implement the step-doubling algorithm to adaptively adjust the step size. If the error of a Runge-Kutta step is greater than the tolerance, the same step is repeated with half the step size. Alternatively, if the error is less than half of the tolerance, the step size is doubled for the next calculation. Finally, if the step size is greater than the distance to the next measurement, that distance is used as the step size, using the normal value afterwards. Otherwise, the algorithm proceeds with the consistent step size.

To calculate the error, we compare one lattice $\vec{e}_1$ produced using a step of size $2h$ with another lattice $\vec{e}_2$ produced via two steps of size h. The error Δ can be estimated to up the fifth order of h as [**?**]

$$\Delta = \frac{1}{15}\sqrt{\sum_x |\vec{e}_2(x) - \vec{e}_1(x)|} \tag{8}$$

The tolerance used in this work is $\Delta_{max} = 0.01$.

4. Results

References

[1] C. Callan, D. Friedan, E. Martinec and M. Perry, *Strings in background fields*, .

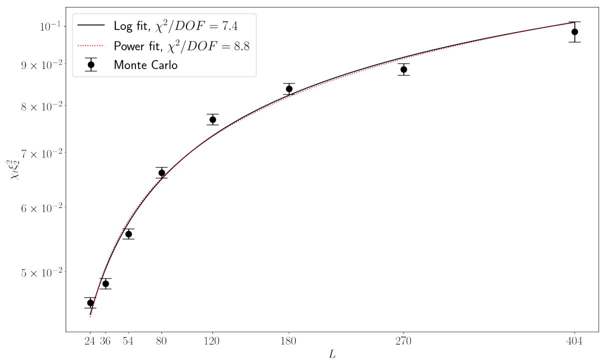

(**a**) $\tau = 0$

(**b**) $\tau = 5t_0$

Figure 3: $\chi_t \xi_2^2$ as a function of L. ξ_2 is the second moment of the correlation function and t_0 is a scale-independent unit of flow time. We fit the data with both a logarithmic and power fit. Simulation run with 10,000 measurements every 50 sweeps, 1,000 sweep thermalization. In the $\tau = 0$ case, we have compared our result with the curve fits found in [6].

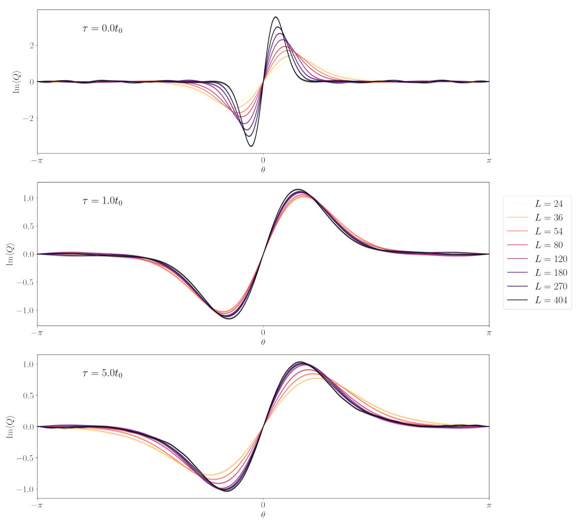

Figure 4: Nontrivial $\mathrm{Im}\langle Q \rangle$ as a function of θ. Simulation run with 10,000 measurements, every 50 sweeps, 1,000 sweep thermalization. Note the different scaling of the y-axis.

[2] A. Polyakov, *Interaction of goldstone particles in two dimensions. Applications to ferromagnets and massive Yang-Mills fields*, .

[3] P. Goddard and P. Mansfield, *Topological structures in field theories*, .

[4] A.Y. Kitaev, *Quantum computations: Algorithms and error correction*, .

[5] B. Berg and M. Lüscher, *Definition and statistical distributions of a topological number in the lattice $O(3)$ σ-model*, .

[6] W. Bietenholz, P. de Forcrand, U. Gerber, H. Mejía-Díaz and I.O. Sandoval, *Topological Susceptibility of the 2d O(3) Model under Gradient Flow*, 1808.08129.